Elimination of Phosphorylation Sites of Semliki Forest Virus Replicase Protein nsP3*

Received for publication, July 11, 2000, and in revised form, December 1, 2000
Published, JBC Papers in Press, December 4, 2000, DOI 10.1074/jbc.M006077200

Helena Vihinen‡§, Tero Ahola‡¶, Minna Tuittila‖, Andres Merits‡, and Leevi Kääriäinen‡***

From the ‡Program in Cellular Biotechnology, Institute of Biotechnology, Viikki Biocenter, P. O. Box 56, University of Helsinki, FIN-00014 Helsinki, and the Department of Biochemistry and Pharmacy, Åbo Academi University, 20500 Turku Finland

nsP3 is one of the four RNA replicase subunits encoded by alphaviruses. The specific essential functions of nsP3 remain unknown, but it is known to be phosphorylated on serine and threonine residues. Here we have completed mapping of the individual phosphorylation sites on Semliki Forest virus nsP3 (482 amino acids) by point mutational analysis of threonine residues. This showed that threonines 344 and 345 represented the major threonine phosphorylation sites in nsP3. Experiments with deletion variants suggested that nsP3 itself had no kinase activity; instead, it was likely to be phosphorylated by multiple cellular kinases. Phosphorylation was not necessary for the peripheral membrane association of nsP3, which was mediated by the N-terminal region preceding the phosphorylation sites. Two deletion variants of nsP3 with either reduced or undetectable phosphorylation were studied in the context of virus infection. Cells infected with mutant viruses produced close to wild type levels of infectious virions; however, the rate of viral RNA synthesis was significantly reduced in the mutants. A virus totally defective in nsP3 phosphorylation and exhibiting a decreased rate of RNA synthesis also exhibited greatly reduced pathogenicity in mice.

Phosphorylation and dephosphorylation have been recognized as major processes by which protein function is regulated. A wide range of proteins display phosphorylation state-dependent activity, including proteins involved in signal transduction, transcription, and the cell cycle. In the field of RNA virus replication, the phosphoprotein P of negative-strand RNA viruses with unsegmented genomes such as rhabdoviruses (order Mononegavirales) has a central function in regulating viral mRNA transcription and possibly RNA replication (1).

The alphaviruses are a globally distributed group of enveloped positive-strand RNA animal viruses capable of causing fatal encephalitis; representative members include Sindbis virus (SIN)[1] and Semliki Forest virus (SFV). The RNA synthesis of alphaviruses occurs in the cytoplasm, where the 5′ two-thirds of the genomic RNA (total length, ~11.5 kilobases) is translated into a large polyprotein of ~2500 amino acids (aa). This polyprotein, termed P1234, is autoproteolytically cleaved to yield the four subunits of the viral RNA-dependent RNA polymerase, the nonstructural proteins nsP1–nsP4 (reviewed in Refs. 2 and 3). Polyprotein processing intermediates have distinct essential functions during the early phase of RNA replication, the synthesis of negative strands (4–6). Later in infection, the negative strands are used as stable templates for synthesis of progeny-positive strands, and for synthesis of subgenomic mRNAs coding for the structural proteins of the virus.

nsP1 is an enzyme responsible for methylation and capping of viral mRNAs (7, 8). In addition, it mediates membrane association of the RNA replication complex (9) and its targeting onto the cytoplasmic surface of endosomes and lysosomes (10). nsP2 is an RNA helicase (11), RNA triphosphatase (12), and an autoprotease responsible for the cleavage of the nonstructural polyprotein (3). nsP4 is the catalytic subunit of this RNA-dependent RNA polymerase (13). Each of these three polypeptides has conserved amino acid sequence motifs, when compared with cellular and viral proteins of similar function: nsP4 with RNA-dependent polymerases, nsP2 with nucleic acid helicases and papain-like cysteine proteases, and nsP1 with methyltransferases (14, 15).

In contrast, the functions of nsP3 are not well defined, although the protein is essential for RNA replication (16). Studies of temperature-sensitive and linker insertion mutants of SIN nsP3 have implicated it in negative-strand RNA synthesis, and possibly also in the synthesis of subgenomic mRNA (6, 17). The amino acid sequence of SFV nsP3 (482 aa) can be divided into three almost equal sections. The first third forms a small domain conserved in alphaviruses, rubella virus, hepatitis E virus, and coronaviruses (14). Recently, through genome sequencing, it has become apparent that this domain is widely, although not universally distributed in bacteria, archae, and eukaryotes. It usually exists on its own as a small open reading frame, but a more divergent version can be found attached to unusual histone variants, the macrohistones H2A (18). For the moment, this unanticipated conservation imparts little insight, since none of the nsP3-related proteins have been functionally characterized. The middle third of nsP3 is only conserved between alphaviruses, whereas the last third (after Tyr^{324}; Fig. 1) is hypervariable, showing no discernible conservation. Even

* This work was supported in part by Academy of Finland Grant 8397 and by grants from the Technology Development Center and Helsinki University Foundation. The costs of publication of this article were defrayed in part by the payment of page charges. This article must therefore be hereby marked "*advertisement*" in accordance with 18 U.S.C. Section 1734 solely to indicate this fact.

¶ Present address: Pfizer Global Research and Development, Sandwich, Kent, United Kingdom.

§ To whom correspondence should be addressed: Inst. of Biotechnology, P.O. Box 56, Viikinkaari 9, University of Helsinki, Helsinki FIN-00014, Finland. Tel.: 358-9-191-59650; Fax: 358-9-191-59560; E-mail: helena.vihinen@helsinki.fi.

** Biocentrum Helsinki fellow.

[1] The abbreviations used are: SIN, Sindbis virus; SFV, Semliki Forest virus; nsP, nonstructural protein; BHK, baby hamster kidney; PFU, plaque-forming unit; PBS, phosphate-buffered saline; p.i., postinfection; CK II, casein kinase II; PAGE, polyacrylamide gel electrophoresis; aa, amino acid(s); MES, 4-morpholineethanesulfonic acid.

the size of this C-terminal "tail" varies in different alphaviruses: SFV nsP3 has 158 aa and SIN nsP3 232 aa (3). The tail is rich in acidic residues, as well as in serine, threonine, and proline, and devoid of predicted secondary structure.

nsP3 is the only alphavirus nonstructural protein modified by phosphorylation (19, 20). Phosphoamino acid analysis of SFV nsP3 showed that serine and threonine residues are phosphorylated, approximately in 2:1 ratio, whereas no phosphotyrosine could be found (19). The major phosphorylation sites of SFV nsP3 were determined by mass spectrometric analysis in conjugation with on-target alkaline phosphatase digestion, as well as two-dimensional peptide mapping and Edman sequencing (21). In SFV nsP3 the serines 320, 327, 332, and 335 and from 7 to 12 residues in peptide Gly^{338}–Lys^{415} can be phosphorylated. SIN nsP3 is even more heavily phosphorylated on serine and threonine, leading to formation of several species of different electrophoretic mobility (20). Deletions in the nonconserved tail region of SIN nsP3 considerably reduce its phosphorylation, suggesting that the modification may primarily occur in this part of the protein (22). nsP3 is capable of associating with cellular membranes when expressed alone (23).

Here we have constructed truncated and point-mutated derivatives of SFV nsP3 and studied their phosphorylation. This enabled the introduction of phosphorylation-defective nsP3 variants to the SFV genome, to better understand the role of phosphorylation of nsP3 in the alphavirus life cycle. The resultant mutant viruses were characterized in cell culture with respect to growth and RNA synthesis. Finally, a virus encoding nonphosphorylated nsP3 was used in studies of neurovirulence in mice.

EXPERIMENTAL PROCEDURES

Plasmids and Plasmid Construction—Deletions and point mutations were made in SFV *nsp3* present in plasmid pTSF3 under the T7 promoter (24). The C-terminal *nsp3* deletion mutant Δ329–482 (*N-nsp3*, Fig. 1) was generated by PCR utilizing downstream primer 1 (see list of primers below), and upstream primer 2. The PCR product was cloned into *Nco*I/*Hin*dIII-digested pTSF3. The internal *nsp3* deletion *Δ343–368* was made using PCR with primer pairs 2 and 3, and 4 and 5. The PCR products were purified (Qiagen PCR purification kit) and used as a template in a second PCR with primers 2 and 4. The internal deletion construct *nsp3Δ319–368* was made using primers 6 and 7 together with primers 2 and 4 as described for *nsp3Δ343–368*. The C-terminal construct *nsp3Δ1–311* (*C-nsp3*) was made using primers 8 and 2. Selected serine and threonine residues were mutated to alanine by using the unique site elimination mutagenesis kit (Amersham Pharmacia Biotech) according to the manufacturer's instructions. All deletions and point mutations were verified by DNA sequencing. The deletions *nsp3Δ319–368* (*nsp3Δ50*) was cloned into the infectious cDNA (pSP6-SFV4; Ref. 25) via an intermediate clone containing the *Sac*I/*Bgl*II fragment of the infectious cDNA clone in vector pSP73 (Promega).

Primers 1–8 were constructed as follows: primer 1, 5′-CTCAAGCTTACGTAGATGCGGCATACTTCCGCGG-3′; primer 2, 5′-CTCAAGCTTATGCACCCGCGCGGCCTAGTCG-3′; primer 3, 5′-ATCACCATGGCACCATCCTACAGAGTTAAG-3′; primer 4, 5′-TCGTAGTCCAAGTCAAACCCTCGTAACGACCGATC-3′; primer 5, 5′-TGGACTACGAGCCAATGGCTCCCATAGTAGTGACGG-3′; primer 6, 5′-CAGTGTACGAGCCAATGGCTCCCATAGTAGTGACGG-3′; primer 7, 5′-TCGTACACTGAAGGTACCGTCGGGACGAACAGG-3′; and primer 8, 5′-ATCCATATGACCATGGACCCGACGGTACCTTCAGTGG-3′.

Cells and Viruses—HeLa cell monolayers were grown in Dulbecco's modified minimal essential medium supplemented with 10% heat-inactivated fetal bovine serum and 100 units/ml streptomycin and penicillin. The modified recombinant vaccinia virus Ankara was kindly provided by Dr. Moss (National Institutes of Health, Bethesda, MD), and stock was grown in baby hamster kidney (BHK) cells as described (26). Propagation of the SFV strain and cultivation of BHK and Vero cells have been described previously (27).

Protein Expression in HeLa Cells—HeLa cells (80–90% confluent) were infected with modified vaccinia Ankara using 20–50 plaque-forming units (PFU)/cell. After a 45-min adsorption period, the cells were washed and transfected in OptiMEM (Life Technologies, Inc.) with pTSF3 or its derivatives, using Lipofectin (Life Technologies, Inc.). 7 μg of DNA in 12 μl of Lipofectin, and 10 μg in 50 μl were used for 60- and 100-mm plates, respectively. After 3–4 h the transfection mixture was replaced with normal growth medium containing serum, and the incubation was continued for 1–3 h.

For *in vivo* labeling, transfected cells were washed twice with Dulbecco's medium containing 0.2% bovine serum albumin at 2 h after transfection and a methionine/cysteine-free or a phosphate-free medium was added. Cells were labeled at 3 h after transfection with either 150 μCi of [^{35}S]methionine/cysteine (>1000 Ci/mmol, Redivue PROmix, Amersham Pharmacia Biotech) or 200–500 μCi of carrier-free [^{32}P]orthophosphate (Amersham Pharmacia Biotech) per 100-mm plate. After 3–5 h of labeling, cells were washed carefully, harvested, and lysed in 1% SDS. After shearing the DNA with a syringe and a 27-gauge needle, proteins were denatured by boiling and nsP3 was immunoprecipitated as described below, followed by SDS-PAGE analysis. The radioactive proteins were detected using a Fuji Bas 1500 Bioimaging Analyzer instrument.

Immunoprecipitation, Immunoblotting, and Immunofluorescence—HeLa cells were lysed in phosphate-buffered saline (PBS) containing 1% SDS, 10 mM sodium fluoride (Merck), and protease inhibitor mixture (Complete™; Roche Molecular Biochemicals). After boiling the samples for 2 min, immunoprecipitation was carried out with a polyclonal anti-nsP3 rabbit antiserum as described previously (19). For immunoblotting, the samples, resolved by SDS-PAGE in 10% gels, were transferred to nitrocellulose membrane (Hybond ECL or Hybond-C-extra; Amersham Pharmacia Biotech) as described previously (7). Polyclonal anti-nsP3 rabbit antiserum was used in 1 to 10,000 dilution, polyclonal anti-nsP3 guinea pig antiserum in 1 to 10,000 dilution, and anti-phosphothreonine (Zymed Laboratories Inc.) in 1 to 1,000 dilution. The secondary antibodies were swine-anti-rabbit IgG (Dako) and donkey-anti-guinea pig IgG (Jackson Immunoresearch Laboratories) conjugated to horseradish peroxidase. The proteins were visualized using an enhanced chemiluminescence detection system (Amersham Pharmacia Biotech). Indirect immunofluorescence microscopy was carried out for transfected cells at 4 h after transfection using Bio-Rad MRC1024 confocal microscope. The cells were fixed with 4% paraformaldehyde in cytosolic buffer (10 mM MES, pH 6.0, 138 mM KCl, 3 mM $MgCl_2$, 2 mM EGTA, and 11% sucrose) for 15 min and permeabilized with 0.1% Triton X-100 for 1 min. The cells were labeled with anti-nsP3 antiserum (1:500), followed by donkey rhodamine red X-conjugated anti-rabbit IgG (1:300, Jackson Immunoresearch Laboratories) as a secondary antibody.

Comparison of Virus Growth in BHK, Vero, and NIH Cells—Derivative of the infectious cDNA (pSP6-SFV4) containing nsp3 deletion *nsp3Δ50* was transcribed *in vitro*, and the obtained RNA was used to transfect BHK cells. The cells were incubated overnight (37 °C), and the virus was collected, centrifuged at low speed to remove cell debris, and used to infect fresh BHK cells (100 μl of supernatant to 150 cm^2 cells) to obtain a second virus passage. After overnight incubation the virus was collected and centrifuged at low speed, and 5% of glycerol was added to the virus stock. Virus titers were determined by plaque assay (27). Monolayers of BHK, NIH, or Vero were infected using 50 PFU/cell. At 1 h after infection, the media were changed and the incubation was continued at 37 °C. Samples were taken from the media at 2, 4, 6, 8, 10, and 12 h postinfection (p.i.), and the amount of the virus was determined by plaque formation and hemagglutination assays (27).

Viral RNA Synthesis—BHK cells (2×10^6 cells/35-mm Petri dish) were infected with 50 PFU/cell wild-type SFV, SFV nsP3Δ26, SFV nsP3Δ50, or mock-infected. At 1 h p.i., the virus was removed and the medium including actinomycin D (2 μg/ml) was added. Duplicate dishes of each set were pulse-labeled with 50 μCi/dish for 30 min in the presence of actinomycin D (2 μg/ml) at 1.5, 2.5, 3.5, 4.5, and 5.5 h p.i. At the end of pulse period, monolayer was washed twice with cold PBS and cells were solubilized into buffer containing 0.5% SDS, 10 mM Tris-HCl, pH 7.5, 100 mM NaCl at 65 °C. After shearing the DNA with a 27-gauge needle, the proteins were denatured by boiling. Part of the sample (5%) was used for determining the total protein content (Protein Assay, Bio-Rad), while proteinase K (200 μg/ml, Roche Diagnostics GmbH) and 4 mM $CaCl_2$ was added to the rest of the sample and the samples were incubated at 37 °C for 30 min. The viral RNA in double sets of 200-, 300-, and 400-μl aliquots was precipitated with 10% trichloroacetic acid. After a 30-min incubation on ice, the precipitates were collected onto glass fiber filters (Milllipore AP40), which were washed twice with 5% trichloroacetic acid and dried at 100 °C for 20 min. The incorporated [^{3}H]uridine was quantified by liquid scintillation counting.

Mouse Pathogenicity—Two mouse groups, both consisting of 5 4-to-6 week-old female mice, were infected intraperitoneally with the wild type SFV4 and phosphorylation-deficient mutant SFV nsP3Δ50. The

amount of virus used, determined by plaque assay, was 10^7 PFU in PBS per mouse. Two groups of 10 mice were also infected, with the same dose, for immunohistochemical studies. Two mice were sacrificed daily from 3 days to 7 days after infection. The blood samples were centrifuged at low speed at 4 °C and diluted 1:10 in PBS, and the virus titers were determined as described earlier (27). After perfusing the mice with cold PBS, the brains were divided sagittally. Half of the brain was homogenized in PBS, and supernatant was used for virus titration. For preparation of cryosections, one half of the brain was further divided corollary in two pieces, which were covered with Tissue Tek optimal cooling compound (Miles, IN) and frozen in an isopentane/dry ice bath. The samples were stored in −70 °C until cryosections of 10 μm were prepared on silanized glass. The slices were air-dried, fixed in −20 °C acetone for 10 min, dried, and stored at −20 °C until double-stained with a polyclonal SFVA7(74)-specific antibody (28) using the avidin-biotin-peroxidase detection method (Vectastain ABC kit, Vector Laboratories) and hematoxylin staining for nuclei.

RESULTS

Phosphorylation of Wild Type nsP3 and Deletion Mutant N-nsP3—To study phosphorylation of SFV nsP3, we synthesized the protein in relatively large amounts in eukaryotic cells by transfection. HeLa cells were infected with the attenuated vaccinia virus Ankara, which encodes bacteriophage T7 RNA polymerase (26), followed by transfection with a plasmid encoding nsP3 under the T7 promoter. The cultures were labeled with [^{32}P]orthophosphate from 3 to 6 h after transfection. In preliminary experiments, phosphoamino acid analysis had revealed that the wild type nsP3 was phosphorylated on serine and threonine, as described for the protein synthesized during SFV infection (data not shown; Ref. 19). Next, we expressed the wild type nsP3 and N-nsP3 (nsP3Δ329–482) from which the nonconserved C-terminal region had been deleted (Fig. 1). The transfected and ^{32}P-labeled cells were harvested, and the lysates were subjected to immunoprecipitation with a specific anti-nsP3 antiserum, followed by SDS-PAGE analysis. Both the wild type nsP3 and the truncated derivative N-nsP3 were detected in Western blotting by anti-nsP3 antibodies (Fig. 2*A*, *lanes 3* and *4*). N-nsP3 was poorly labeled with [^{32}P]phosphate (*lanes 1* and *2*), representing only about 1% ^{32}P activity as compared with the wild type. In Western blots, an anti-phosphothreonine antiserum detected the wild type nsP3 but failed to recognize N-nsP3 (Fig. 2*A*, *lanes 5* and *6*). Based on these experiments, the conserved region of nsP3 (aa 1–328) did not contain phosphorylated threonine residues, and it was poorly phosphorylated on serine residues.

The major phosphorylation sites of nsP3 have been determined by mass spectrometric analysis in conjugation with on-target alkaline phosphatase digestion as well as two-dimensional peptide mapping and Edman sequencing (21). At least serines 320, 327, 332, and 335 and from 7 to 12 residues in peptide Gly^{338}–Lys^{415} are potential phosphorylation sites (Fig. 1*B*). However, the mass spectrometric analysis as well as two dimensional peptide mapping and Edman sequencing failed to identify phosphorylated residues in peptide Gly^{338}–Lys^{415}. Therefore, to complete the mapping of SFV nsP3 phosphorylation sites, and to confirm the results of mass spectrometric analysis, we performed point mutational studies and constructed additional deletions.

Phosphorylation of Threonines—To further study the phosphorylated threonine residues of SFV nsP3, we made eight different constructs mutating to alanine all the 11 threonines present in the C-terminal region of nsP3 (Fig. 1*B*), individually or in pairs. All constructs were expressed in HeLa cells as above. Western blotting with anti-nsP3 antiserum showed that the relative amounts of mutant nsP3 proteins were similar to that of the wild type nsP3 (Fig. 2*B*, *lower panel*). Probing a parallel blot with anti-phosphothreonine antiserum revealed that a double mutant T344A/T345A reacted only very weakly,

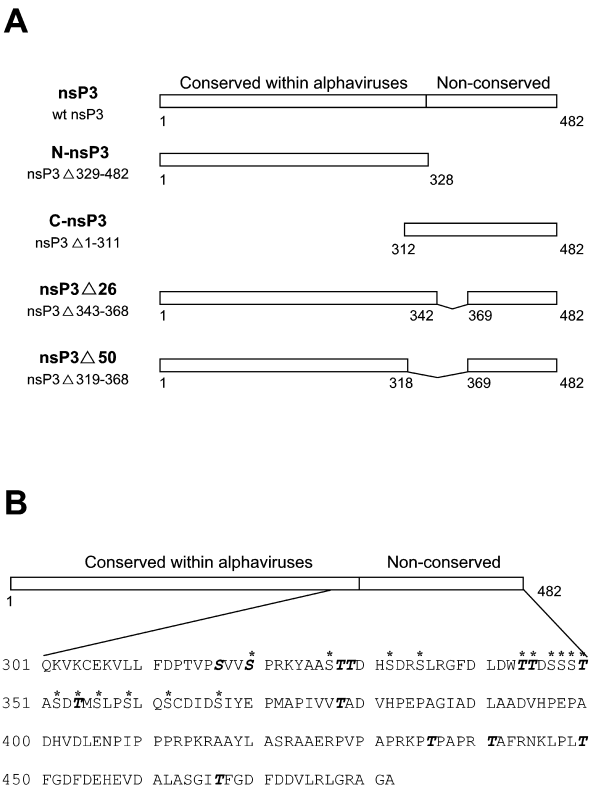

FIG. 1. A, scheme of the SFV nsP3 derivatives used in this work. The conserved and nonconserved regions are marked at the top. The nomenclature of the derivatives, as well as the deleted residues, are indicated on the left. The amino acid residues included in the constructs are shown in the scheme on the right. Internally deleted region regions are denoted by thin lines. B, amino acid sequence of the C-terminal part of SFV nsP3. Residues mutated during the course of this work are shown in boldface, and potentially phosphorylated residues (21) are marked with asterisks above the residues.

whereas other mutants retained approximately wild type levels of threonine phosphorylation (Fig. 2*B*, *upper panel*). When Thr^{344} and Thr^{345} were mutated separately to alanine and the resulting derivatives expressed in HeLa cells, repeated experiments indicated that both threonines were needed for efficient phosphorylation of this site (Fig. 2*B*, *lower panel*, *lanes 10* and *11*). Mass spectrometric analysis has revealed that tryptic peptide Gly^{338}–Lys^{415} carried from 7 to 12 phosphates (21). Thus, in proteins carrying 12 phosphates, threonines 350 and 354 were also phosphorylated (assuming that phosphorylation of Thr^{378} could be excluded based on phosphorylation studies of deletion mutant nsP3Δ50, see below). However, double mutation of Thr^{350} and Thr^{354} did not show decreased reaction with anti-phosphothreonine antiserum (Fig. 2), indicating that the major phosphothreonines in SFV nsP3 were Thr^{344} and Thr^{345}. Mutating either threonine alone appeared to decrease phosphorylation to a degree almost similar to the double mutation, and either or both of them could be phosphorylated in the wild type nsP3. It is noteworthy that the phosphorylated threonine residues were in close vicinity of the phosphorylated serines, indicating that a small subregion of nsP3 contained large majority of the phosphorylated residues (Fig. 1*B*).

Phosphorylation of C-terminal Peptide (aa 312–482)—To study whether full-length nsP3 was needed either to provide appropriate conformation and/or kinase activity to phosphorylate the serines/threonines in region 320–368, we made a deletion construct where the N-terminal first two thirds of nsP3 were removed (C-nsP3, nsP3Δ1–311; Fig. 1*A*). Anti-nsP3 antiserum was able to recognize this C-terminal peptide expressed

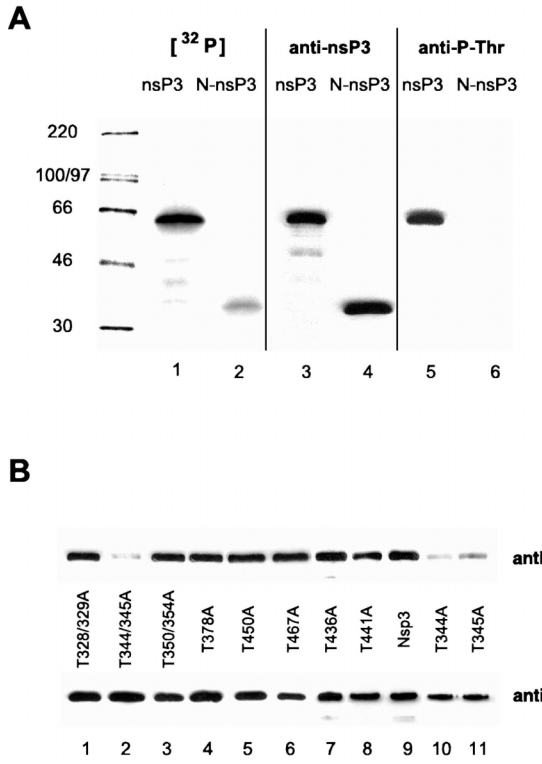

FIG. 2. **Threonine phosphorylation of nsP3.** *A*, the full-length nsP3 or the N-terminal portion N-nsP3 were expressed in HeLa cells by transfection, and the cells were labeled with [^{32}P]orthophosphate. Cell extracts either were immunoprecipitated with anti-nsP3 antibodies and analyzed by SDS-PAGE and autoradiography to detect labeling or were analyzed by Western blotting with anti-nsP3 or anti-phosphothreonine antibodies, as indicated at the *top*. Molecular mass markers (in kDa) are shown on the *left*. *B*, the indicated point mutated derivatives of nsP3 were expressed in HeLa cells. Cell extracts were analyzed by Western blotting with anti-phosphothreonine (*upper panel*) and anti-nsP3 (*lower panel*) antibodies.

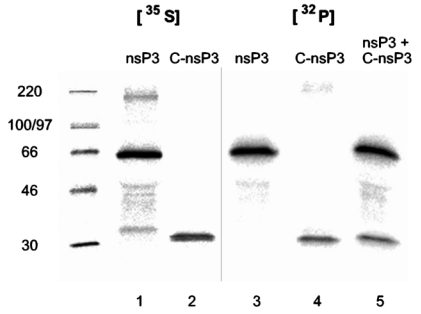

FIG. 3. **Phosphorylation of nsP3 and C-nsP3.** nsP3 and its C-terminal domain C-nsP3 were expressed in HeLa cells. The cells were labeled with either [^{32}P]orthophosphate or [^{35}S]methionine/cysteine as indicated at the *top*. Cell extracts were immunoprecipitated with anti-nsP3 antibodies and analyzed by SDS-PAGE and autoradiography. Molecular mass markers (in kDa) are shown on the *left*.

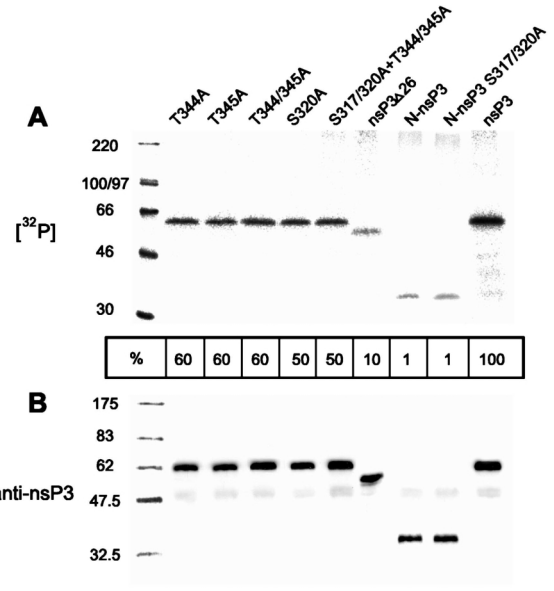

FIG. 4. **Phosphorylation of nsP3 derivatives.** The nsP3 derivatives indicated at the *top* were expressed in HeLa cells. The cells were labeled with [^{32}P]orthophosphate, and cell extracts were analyzed by immunoprecipitation with anti-nsP3 rabbit antiserum and autoradiography to detect labeling (*A*) or by Western blotting with anti-nsP3 guinea pig antiserum to verify the level of expression (*B*). The *numbers below panel A* indicate the amount of phosphorus labeling as normalized with respect to the wild type nsP3.

in HeLa cells by transfection (Fig. 3, *lane 2*). This peptide could be labeled with [^{32}P]orthophosphate (Fig. 3, *lane 4*). According to metabolic labeling with [^{35}S]methionine and [^{32}P]orthophosphate the degree of phosphorylation of C-nsP3 was about 30% of that of the full-length protein. This difference may be due to altered conformation of the peptide. Alternatively, the subcellular localization of C-nsP3 may be different from that of the full-length protein, which might make it differentially accessible to kinases. To study the possibility of nsP3 autophosphorylation, the C-terminal peptide was cotransfected with the wild type nsP3. No increase in the phosphorylation level of C-nsP3 was detected (Fig. 3, *lane 5*). Since it is unlikely that the variable C-terminal region with an unusual amino composition would have kinase activity, our results suggest that the phosphorylation of C-nsP3 and the wild type nsP3 is catalyzed by cellular kinases.

Effects of Point Mutations and Deletions on the Phosphorylation of nsP3—To study the phosphorylation of individual amino acids, we made various point mutations in nsP3 and N-nsP3, expressed the mutated derivatives in HeLa cells by transfection, and labeled the proteins with [^{32}P]orthophosphate. The expression level was determined by Western blotting with anti-nsP3 antiserum (Fig. 4*B*), and the ability of the mutant proteins to incorporate [^{32}P]orthophosphate was compared with that of wild type nsP3 (Fig. 4*A*). The total phosphorylation level of the T344A/T345A threonine double-mutant was ~40% less than that of the wild type nsP3, as quantified with a phosphorimager (Fig. 4, *lanes 3* and *9*). When either of the threonines 344 or 345 was singly mutated, a similar decrease in phosphorylation was observed (Fig. 4, *lanes 2* and *3*). Mutation of Ser^{320}, which in mass spectrometric analysis seemed to be one of the major serine phosphorylation sites, also decreased the phosphorylation degree of nsP3 by ~50% (Fig. 4, *lane 4*). However, when mutations T344A/T345A and S320A were combined, no further decrease in phosphorylation was observed (Fig. 4, *lane 5*). These results suggest that the different phosphorylation sites may influence each other in a rather complex manner, and therefore phosphorylation of individual sites cannot be simply quantified based on point mutational studies. The phosphorylation level of N-nsP3 was about 1% as compared with the wild type (Fig. 4, *lane 7*), as already seen in Fig. 2*A*. Mutation of Ser^{317} and Ser^{320} did not greatly affect the phosphorylation level of N-nsP3 (Fig. 4, *lane 8*), suggesting that it is phosphorylated on the remaining known site Ser^{327} (Fig. 1*B*). A small internal deletion of 26 amino acids, nsP3Δ26 (nsP3Δ343–368; Fig. 1*A*), reduced nsP3 phosphorylation by 90% (Fig. 4, *lane 6*).

Next, we wanted to generate a nsP3 derivative, in which all

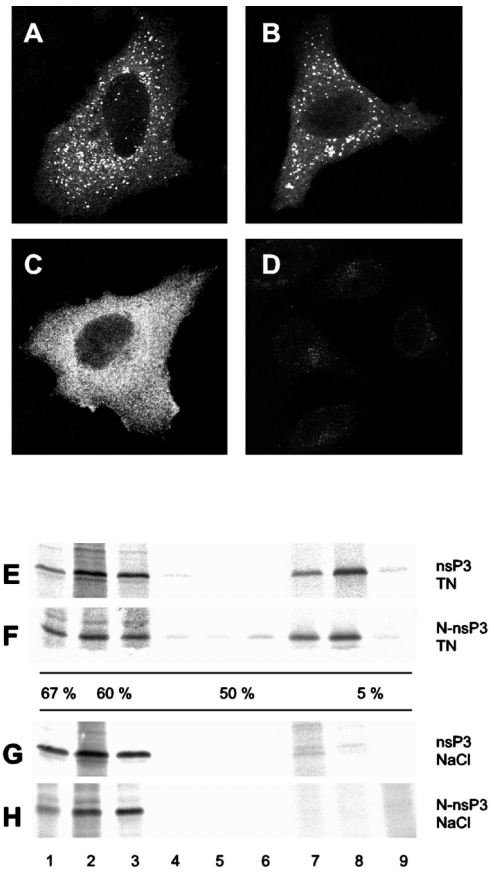

FIG. 5. **Membrane association and localization of nsP3 and its derivatives.** *A–D*, HeLa cells expressing wild type nsP3 (*A*), nsP3Δ50 (*B*), C-nsP3 (*C*), or mock-transfected HeLa cells (*D*) were fixed at 4 h after transfection and subjected to immunofluorescent labeling with anti-nsP3 antiserum. *E–H*, HeLa cells expressing the wild type nsP3 or the truncated derivative N-nsP3 were broken by Dounce homogenization (8), and the extracts were analyzed in discontinuous sucrose gradients consisting of 67%, 60%, 50%, and 5% (w/w) layers in 100 mM NaCl, 50 mM Tris, pH 7.5 (*E* and *F*), or in the same buffer containing 500 mM NaCl (*G* and *H*). The samples were adjusted to 60% (w/w) sucrose and loaded on top of the 67% layer. During centrifugation (Beckman SW50.1 rotor at 35,000 rpm for 16 h), membrane-associated material floated to the interface of 50% and 5% layers (9).

the known phosphorylation sites of nsP3 would be eliminated. In this construct 50 aa were deleted, removing the entire phosphorylated region (nsP3Δ50; Fig. 1*A*). The construct was expressed in transfected HeLa cells at levels similar to the wild type nsP3, and did not incorporate detectable amounts of [^{32}P]orthophosphate (see below).

Effect of Phosphorylation on Membrane Association of nsP3—In SFV-infected BHK cells, nsP3 is associated with modified endosomes and lysosomes (29). When nsP3 is expressed alone in mammalian cells by transfection, it can also be found in vesicular and vacuolar structures in the cytoplasm (23). It has been suggested previously that there could be a connection between phosphorylation and membrane association of nsP3 (19). To further examine this issue, we studied the localization of transfected nsP3 derivatives by indirect immunofluorescence. Both the wild type nsP3 (Fig. 5*A*) and the nonphosphorylated derivative nsP3Δ50 (Fig. 5*B*) were associated with vesicular structures in HeLa cells. Therefore, phosphorylation of nsP3 is not needed for its ability to associate with these structures. In contrast, the phosphorylated C-terminal peptide C-nsP3 showed a diffuse cytoplasmic distribution (Fig. 5*C*), indicating that it does not contain determinants for membrane association.

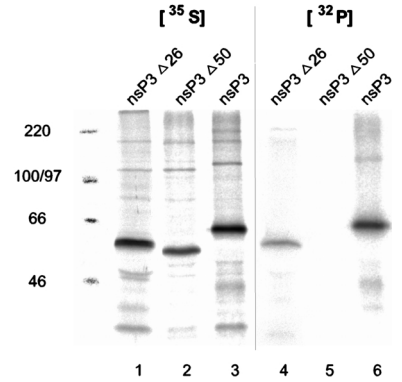

FIG. 6. **Phosphorylation of nsP3 and its derivatives in SFV-infected cells.** BHK cells were infected with viruses encoding wild type nsP3 or its mutated derivative nsP3Δ26 or nsP3Δ50, as indicated at the *top*. The cells were labeled with [^{35}S]methionine/cysteine (*lanes 1–3*) or [^{32}P]orthophosphate (*lanes 4–6*). Cell extracts were collected, immunoprecipitated with anti-nsP3 antibody, and analyzed by SDS-PAGE and fluorography. Molecular mass markers (in kDa) are shown on the *left*.

To study the membrane association of nsP3 biochemically, extracts of cells expressing the wild type nsP3 or the truncated derivative N-nsP3 were floated in a discontinuous sucrose gradient. Approximately one third of both nsP3 and N-nsP3 floated with membranes in low salt buffer (Fig. 5, *E* and *F*). Since N-nsP3 is minimally phosphorylated, phosphorylation does not contribute to the membrane association of nsP3. Instead, the biochemical determinants of membrane association are located within the conserved N-terminal region of nsP3. The association of nsP3 and N-nsP3 with membranes was peripheral in nature, since both proteins were efficiently solubilized by 0.5 M NaCl (Fig. 5, *G* and *H*).

nsP3 Deletion Mutants in SFV Infection—To study the effect of nsP3 phosphorylation in the natural context of SFV infection, we introduced the segments coding for the 26- and 50-aa deletion mutants of nsP3 into the infectious cDNA clone of SFV. *In vitro* transcribed full-length viral RNAs were used to transfect BHK cells, which led to visually observed cytopathic effect, indicating that the mutant constructs generated infectious viruses. As a control we transcribed wild type icDNA of SFV4. Cell supernatants were used to grow second-generation virus stocks, which were plaque-titrated. The titers of the viruses were 7×10^8 PFU/ml for SFV nsP3Δ26, and 3×10^9 PFU/ml for SFV4 and SFV nsP3Δ50. BHK cells were infected with these viruses using 50 PFU/cell, and the cells were labeled with [^{35}S]methionine/cysteine and [^{32}P]orthophosphate. nsP3 was immunoprecipitated from the cell lysates using anti-nsP3 antiserum. The mutant viruses produced nsP3 of the expected size (Fig. 6, *lanes 1–3*) but comparing to the wild-type SFV nsP3 only 10% of [^{32}P]orthophosphate was incorporated to mutated nsP3 produced in SFV nsP3Δ26 infection (Fig. 6, *lanes 5* and *6*). Moreover, no detectable amounts of [^{32}P]orthophosphate was incorporated to the mutated nsP3 in SFV nsP3Δ50 infection (Fig. 6, *lane 4*), showing that the mutant viruses possessed the expected nsP3 phosphorylation phenotypes.

The efficiencies of virus replication for the wild type SFV and the mutant viruses were compared in one-step growth experiments in BHK, Vero, and NIH cells using 50 PFU/cell for infection. Plaque assays of samples collected at different time points from cells infected with mutant viruses SFV nsP3Δ26 and SFV nsP3Δ50 showed titers similar to wild type SFV in BHK and Vero cells (Fig. 7*A*). In NIH cells the mutated virus titers were 1 order of magnitude lower at 2–12 h p.i. However, after 23 h p.i., the titers of the mutated viruses were similar to the wild-type SFV (Fig. 7*A*). This indicates that nsP3 phospho-

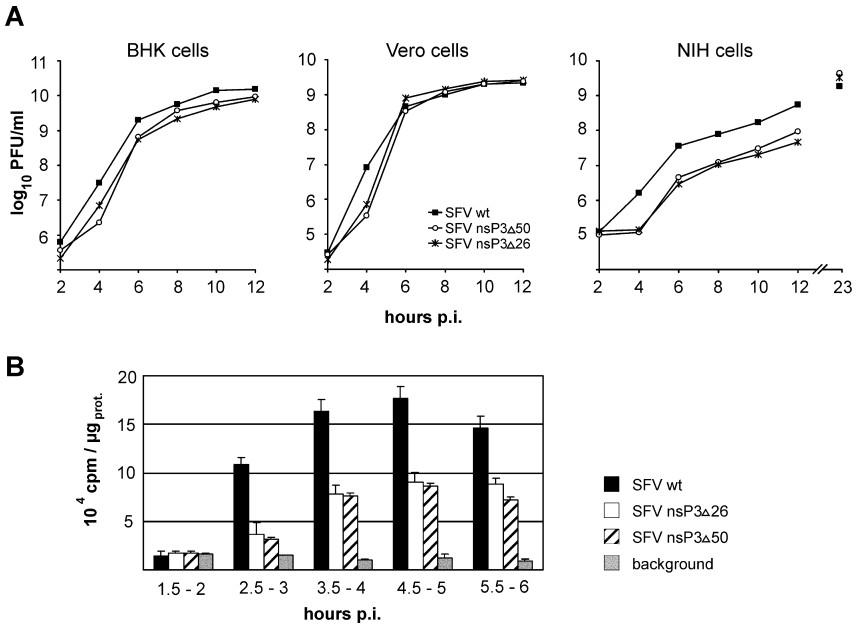

FIG. 7. **Comparison of virus growth in BHK, Vero, and NIH cells and synthesis of viral RNA in BHK cells.** *A*, for growth curves, cells were infected with wild-type SFV, SFV nsP3Δ26, and SFV nsP3Δ50 using 50 PFU/cell at 37 °C. Samples from media were taken at 2, 4, 6, 8, 10, and 12 h p.i., and titrated on BHK cells. *B*, for analysis of viral RNA synthesis, BHK cells were infected with the indicated virus using 50 PFU/cell and labeled with [^{3}H]uridine for 30 min in the presence of actinomycin D. The RNA was precipitated with 10% trichloroacetic acid and quantified by liquid scintillation. The values shown represent the average of three parallel samples; *bars* indicate S.D.

rylation did not greatly increase infectious SFV production in these cell types. However, since a small difference in growth rate could be seen at 4 h p.i. also in BHK and Vero cells, we investigated the level of virus-specific RNA synthesized in BHK cells in early infection. For this, BHK were infected with wild type and mutated viruses using 50 PFU/cell and the viral RNA was metabolically labeled for 30 min at different time points. As shown in Fig. 7*B*, the virus-specific RNA levels of both deletion mutants were significantly reduced at early stages of infection.

Reduced Pathogenecity of nsP3 Phosphorylation-defective Mutant Virus—To study the effects of nsP3 phosphorylation in an animal system, mice were injected intraperitoneally with 10^7 PFU of wild type or nsP3 phosphorylation-defective virus, SFV nsP3Δ50. As described above, this phosphorylation-deficient mutant was able to propagate in BHK, Vero, and NIH cells to titers as high as the wild type SFV. However, this mutant virus was avirulent for mice, since none of the 5 animals infected with SFV nsP3Δ50 was killed or had clinical symptoms during the 3 weeks follow-up period. All five mice infected with the same dose of the wild type SFV (10^7 PFU) died within 6 days. Histochemical analysis revealed that 4 days after infection wild type SFV was widely spread within the brain (both in cerebellum and cerebrum) of the mice having severe paralysis (Fig. 8, *A*, *B*, and *E*). The virus titers of the wild type SFV in the brain of the mice after 5 and 6 days p.i. were 3×10^6 PFU/g of brain and 5×10^6 PFU/g of brain, respectively. In contrast, when mice were infected with SFV nsP3Δ50 mutant virus, no staining of virus structural proteins could been seen in the central nervous system of 6 individual mice. In the brains of 2 mice, isolated viral foci were observed in cerebellum (Fig. 8, *C* and *D*) and cerebrum (Fig. 8*F*). The focal replication of SFV nsP3Δ50 was associated with perivascular areas as shown for cerebellum (Fig. 8*D*). The titer of SFV nsP3Δ50 5 days after infection in the brain of 1 mouse was 3×10^3 PFU/g of brain, and virus titers in the brains of the other 7 mice were under the detection limit between days 4 and 7 after infection. Thus, the nsP3 phosphorylation-defective mutant virus had greatly reduced neurovirulence for adult mice.

DISCUSSION

In this study, we have completed the identification of the main phosphorylation sites of SFV nsP3 by showing that the major threonines phosphorylated are Thr^{344} and/or Thr^{345} (Fig. 2). Several serine residues between amino acids 320 and 368 were also phosphorylated, possibly in a heterogeneous manner. Thus, all the identified phosphorylation sites were concentrated in a small, highly phosphorylated region (Fig. 1*B*). Mutation of one or more serines/threonines affected the phosphorylation of other residues, since the effects of point mutations were not additive (Fig. 4). Specifically, mutation of either Thr^{344} and Thr^{345} or Ser^{320} reduced the overall phosphorylation level of nsP3 by 40–50%, but combination of these two mutations gave no additional reduction. The phosphorylated region was located in the beginning of the nonconserved C-terminal "tail" region of nsP3 (Fig. 1), extending slightly into the conserved domain, as Ser^{320} could be phosphorylated. However, this serine is not conserved among alphaviruses, and thus there appear to be no conserved phosphorylation sites shared by nsP3s from different alphaviruses. Nevertheless, the general feature of extensive phosphorylation of the tail seems to be shared with SIN nsP3 (22).

Among alphaviruses, the nsP3 variable region differs in length and in composition (3). General similarities in the nonconserved regions of alphavirus nsP3s include the presence of proline-rich and acidic regions, which, however, show variation in length and distribution. In the SFV nsP3 nonconserved region, there are two acidic domains: aa 340–406 (15 Asp+Glu in 67 aa, 22%), and aa 453–473 (8 Asp+Glu in 21 aa, 38%) separated by a proline-rich stretch between aa 408–439 (11 prolines in 32 aa, 34%). Most of the phosphorylated sites of SFV nsP3 were in the first acidic region (Fig. 1*B*), making it even more negatively charged. It remains to be determined whether phosphorylation is concentrated in a small subregion of nsP3 also in other alphaviruses. Both acidic and proline-rich domains have been suggested to be consensus motifs for transcriptional activation domains (30, 31).

The C-terminal region of nsP3 (C-nsP3; Fig. 1*A*) was capable of becoming phosphorylated when expressed alone, although at reduced level as compared with the full-length protein (Fig. 3). This reduced phosphorylation may reflect a different conformation leading to differential kinase recognition. Coexpression with the wild type nsP3 did not increase the phosphorylation of the C-terminal peptide, indicating that the N-terminal portion is unlikely to contribute any kinase activity itself. The N-

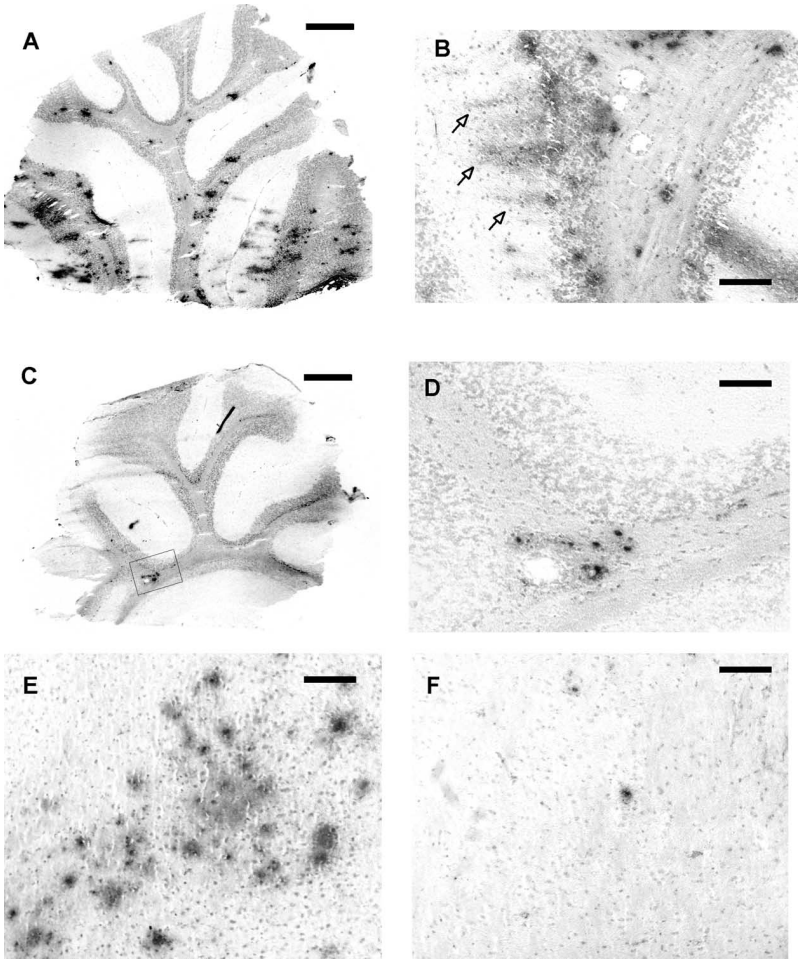

FIG. 8. **Immunoperoxidase staining of brains from mice infected with SFV4 (*A*, *B*, and *E*) and SFV nsP3Δ50 (*C*, *D*, and *F*) 5 days after intraperitoneal infection of 10^7 PFU/mouse.** Staining with hematoxylin and polyclonal anti-SFV antibodies was followed by avidin-biotin peroxidase staining. *A*, general infection of neuronal cells in cerebellum. *B*, a larger magnification of cerebellar region of infected Purkinje cells with antigen-positive dendritic region (*arrows*). *C*, a cluster of SFV nsP3Δ50 infected cerebellar cells in perivascular region shown enlarged in *D*). *E*, multiple infected foci in SFV4 infected cerebrum. *F*, isolated focus in cerebrum of mutant virus-infected mouse. *Bars*, 500 μm in *A* and *C*; 100 μm in *B* and *D–F*.

terminal domain is related to a large protein family with unknown function, but unrelated to known kinases (18). An alternative explanation for the reduced phosphorylation of C-nsP3 is offered by the fact that it was localized in the cytoplasm, whereas the wild type nsP3 was associated with vesicular structures. Thus, C-nsP3 might not be equally accessible to membrane-associated kinases, which may play a role in phosphorylation of the wild type nsP3 since membrane-associated nsP3 is more heavily phosphorylated than soluble nsP3 (19). The phosphorylation of nsP3 was, however, not required for its peripheral membrane association.

Casein kinase II (CK II) has been suggested to be the host enzyme phosphorylating SIN nsP3 (20), based on an experiment in which nsP3 was immunoprecipitated from SIN-infected cells and phosphorylated *in vitro* by a kinase present in the precipitate. The properties of this kinase resembled those of CK II, as assessed by heparin inhibition, polyamine activation, and use of both ATP and GTP as substrate (20). However, the SIN nsP3 studied in this experiment was most likely already phosphorylated within the cells. This may have favored the binding of, and phosphorylation by CK II, which recognizes serines/threonines followed by acidic residues, including phosphorylated residues (32). Thus, CK II is one of the kinases involved in nsP3 phosphorylation, but there are likely to be others. In SFV nsP3, phosphorylation sites at Ser^{327} and Ser^{367} are the best potential sites for CKII (preferred recognition sequence (S/T)-*X*-*X*-(D/E)), but phosphorylation of other sites may become possible, if other sites are already phosphorylated by additional kinases (see sequence in Fig. 1*B*). Among SFV nsP3 phosphorylation sites, Ser^{320}, Ser^{332}, and Ser^{335} are potential protein kinase C sites (recognition sequence (S/T)-*X*-(R/K); Ref. 32). SFV nsP3 Ser^{320} is a consensus site also for $p34^{cdc2}$ kinase. Among negative-strand RNA viruses, the phosphoprotein P may also be a substrate for multiple kinases; examples include phosphorylation of canine distemper and measles virus P proteins by CK II and protein kinase C (33, 34), rabies virus P protein by a unique cellular protein kinase and protein kinase C (35), vesicular stomatis virus P protein by CKII and an L protein-associated kinase (36, 37), and Sendai virus P protein by protein kinase C and a proline-directed protein kinase (38, 39).

Mutant viruses coding for truncated forms of SFV nsP3 replicated to high titers in BHK, Vero, and NIH cells (Fig. 7*A*). nsP3 mutant Δ26 had 10% level of phosphorylation remaining as compared with wild type, whereas mutant Δ50 was not detectably phosphorylated. These results indicate that the mutated nsP3 proteins were able to carry out all their essential functions needed for RNA replication and for high rates of virus production. Therefore, these internal deletions in a region that was predicted to be devoid of secondary structure did not cause gross misfolding of the protein.

When used to infect mice, the SFV nsP3Δ50 mutant virus was avirulent even with a dose of 10^7 PFU/mouse. The rate of viral RNA synthesis of this mutant was significantly lower than that of the wild type SFV resulting the decreased virulence in mice. However, it cannot be simply stated that the decreased RNA synthesis rate is caused solely by the lack of phosphorylation of nsP3, since deletion of amino acids around the phosphorylation sites may have made a contribution to this phenomenon. Recent study with an avirulent SFV mutant A7(74) (40) has revealed the importance of nsP3 in the neuropathogenicity of SFV (28). Phosphorylation of nsP3, as well as

fine-tune the replication of alphaviruses in different cell types. Further studies should reveal the role of the phosphorylated C-terminal region of nsP3 in specific interactions with components of the neuronal cells leading to neurovirulence of Semliki Forest virus.

Acknowledgments—We are grateful to Petra Nygårdas (Åbo Academi and Turku Immunology Center, Turku, Finland) for performing the immunohistochemical assays. We also thank Airi Sinkko and Tarja Välimäki for excellent technical assistance and Dr. Marja Makarow for critical reading of this manuscript.

REFERENCES

1. Hwang, L. N., Englund, N., Das, T., Banerjee, A. K., and Pattnaik, A. K. (1999) *J. Virol.* **73,** 5613–5620
2. Kääriäinen, L., Takkinen, K., Keränen, S., and Söderlund, H. (1987) *J. Cell Sci. Suppl.* **7,** 231–250
3. Strauss, J. H., and Strauss, E. G. (1994) *Microbiol. Rev.* **58,** 491–562
4. Lemm, J. A., Rümenapf, T., Strauss, E. G., Strauss, J. H., and Rice, C. M. (1994) *EMBO J.* **13,** 2925–2934
5. Shirako, Y., and Strauss, J. H. (1994) *J. Virol.* **68,** 1874–1885
6. Wang, Y.-F., Sawicki, S. G., and Sawicki, D. L. (1994) *J. Virol.* **68,** 6466–6475
7. Laakkonen, P., Hyvönen, M., Peränen, J., and Kääriäinen, L. (1994) *J. Virol.* **68,** 7418–7425
8. Ahola, T., and Kääriäinen, L. (1995) *Proc. Natl. Acad. Sci. U. S. A.* **92,** 507–511
9. Ahola, T., Lampio, A., Auvinen, P., and Kääriäinen, L. (1999) *EMBO J.* **18,** 3164–3172
10. Peränen, J., Laakkonen, P., Hyvönen, M., and Kääriäinen, L. (1995) *Virology* **208,** 610–620
11. Gomez de Cedrón, M., Ehsani, N., Mikkola, M. L., García, J. A., and Kääriäinen, L. (1999) *FEBS Lett.* **448,** 19–22
12. Vasiljeva, L., Merits, A., Auvinen, P., and Kääriäinen, L. (2000) *J. Biol. Chem.* **275,** 17281–17287
13. Barton, D. J., Sawicki, S. G., and Sawicki, D. L. (1988) *J. Virol.* **62,** 3597–3602
14. Koonin, E. V., and Dolja, V. V. (1993) *Crit. Rev. Biochem. Mol. Biol.* **28,** 375–430
15. Ahola, T., Laakkonen, P., Vihinen, H., and Kääriäinen, L. (1997) *J. Virol.* **71,** 392–397
16. Hahn, Y. S., Strauss, E. G., and Strauss, J. H. (1989) *J. Virol.* **63,** 3142–3150
17. LaStarza, M. W., Lemm, J. A., and Rice, C. M. (1994) *J. Virol.* **68,** 5781–5791
18. Pehrson, J. R., and Fuji, R. N. (1998) *Nucleic Acids Res.* **26,** 2837–2842
19. Peränen, J., Takkinen, K., Kalkkinen, N., and Kääriäinen, L. (1988) *J. Gen. Virol.* **69,** 2165–2178
20. Li, G., LaStarza, M. W., Hardy, W. R., Strauss, J. H., and Rice, C. M. (1990) *Virology* **179,** 416–427
21. Vihinen, H., and Saarinen, J. (2000) *J. Biol. Chem.* **275,** 27775–27783
22. LaStarza, M. W., Grakoui, A., and Rice, C. M. (1994) *Virology* **202,** 224–232
23. Peränen, J., and Kääriäinen, L. (1991) *J. Virol.* **65,** 1623–1627
24. Peränen, J. (1991) *J. Gen. Virol.* **72,** 195–199
25. Liljeström, P., Lusa, S., Huylebroeck, D., and Garoff, H. (1991) *J. Virol.* **65,** 4107–4113
26. Wyatt, L. S., Moss, B., and Rozenblatt, S. (1995) *Virology* **210,** 202–205
27. Keränen, S., and Kääriäinen, L. (1974) *Acta Pathol. Microbiol. Scand. Sect. B* **82,** 810–820
28. Tuittila, M. T., Santagati, M. G., Röyttä, M., Määttä, J. A., and Hinkkanen, A. E. (2000) *J. Virol.* **74,** 4579–4589
29. Froshauer, S., Kartenbeck, J., and Helenius, A. (1988) *J. Cell Biol.* **107,** 2075–2086
30. Ma, J., and Ptashne, M. (1987) *Cell* **48,** 847–853
31. Mermod, N., O'Neill, E. A., Kelly, T. J., and Tjian, R. (1989) *Cell* **58,** 741–753
32. Kennelly, P. J., and Krebs, E. G. (1991) *J. Biol. Chem.* **266,** 15555–15558
33. Das, T., Schuster, A., Schneider-Schaulies, S., and Banerjee, A. K. (1995) *Virology* **211,** 218–226
34. Liu, Z., Huntley, C. C., De, B. P., Das, T., Banerjee, A. K., and Oglesbee, M. J. (1997) *Virology* **232,** 198–206
35. Gupta, A. K., Blondel, D., Choudhary, S., and Banerjee, A. K. (2000) *J. Virol.* **74,** 91–98
36. Barik, S., and Banerjee, A. K. (1992) *Proc. Natl. Acad. Sci. U. S. A.* **89,** 6570–6574
37. Barik, S., and Banerjee, A. K. (1992) *J. Virol.* **66,** 1109–1118
38. Huntley, C. C., De, B. P., and Banerjee, A. K. (1997) *J. Biol. Chem.* **272,** 16578–16584
39. Byrappa, S., Pan, Y.-B., and Gupta, K. C. (1996) *Virology* **216,** 228–234
40. Atkins, G. J., Sheahan, B. J., and Liljeström, P. (1999) *J. Gen. Virol.* **80,** 2287–2297